K-shell ionization during α decay of polonium isotopes and superheavy nuclei

M. B. Trzhaskovskaya
National Research Center "Kurchatov Institute", Petersburg Nuclear Physics Institute, Gatchina 188300, Russia

V. K. Nikulin
Ioffe Physical Technical Institute, St. Petersburg 194021, Russia

(Received 20 October 2015; published 10 March 2016)

The theory of K-shell ionization during α decay of the $_{84}$Po isotopes is considered in detail as a part of our general study of the inner shell ionization probability of heavy and superheavy nuclei. Calculations of K-shell ionization with allowance made for the α-particle tunneling through the atomic Coulomb barrier have been performed in the framework of the fully quantum mechanical treatment developed for the first time by Anholt and Amundsen. Further information is available [Anholt and Amundsen, Phys. Rev. A **25**, 169 (1982)]. As distinct from all previous the K-shell ionization calculations where the Dirac hydrogenlike wave functions have been used, we have found the discrete and continuum electron wave functions in the framework of the relativistic self-consistent Dirac-Fock method. In addition, we have taken into consideration accurately terms associated with the α-particle tunneling. Our exact calculations show that the tunneling contribution to the ionization probability is of great importance while Anholt and Amundsen have asserted that the contribution is small. We have obtained that the K-shell ionization probability during α decay of five isotopes of $_{84}$Po correlate better with the available experimental data providing the tunneling is included in calculations. New calculations for K-shell ionization during α decay of superheavy elements $^{249}_{100}$Fm, $^{253}_{102}$No, $^{272}_{111}$Rg, as well as $^{222}_{86}$Rn are also presented. The data may be of importance in the combined α,γ, and conversion-electron spectroscopy used in the superheavy element synthesis analysis.

DOI: 10.1103/PhysRevC.93.034312

I. INTRODUCTION

In research on the synthesis of superheavy elements, the region of unstable transfermium nuclei ($Z \geqslant 100$) is the most complicated from both experimental and theoretical viewpoints. In experimental studies, combined α,γ, and conversion-electron spectroscopy is applied which makes it possible to investigate the excited-state features, e.g., the level energies and spins of daughter nuclei produced in α decay of unstable nuclei [1,2]. In recent experiments [1], excited states of the nucleus $^{249}_{100}$Fm were populated by the α decay of $^{253}_{102}$No. Relative probabilities of the electron conversion and γ transitions as well as their ratios, that is, the internal conversion coefficients (ICC) were found via use of the coincidence method. The experimental value of ICC in the K shell for an $E1$ transition with an energy of 279 keV in ^{249}Fm was found to be four times larger than the theoretical value [3]. This anomalous value of ICC generated a need for revision of the existing view of the structure of the nucleus $^{249}_{100}$Fm and its excited states. At present there is no unambiguous answer.

The prime objective of our study is to get basic information on the effect of inner shell ionization during the α decay of superheavy nuclei to investigate its influence on the spectra of internal conversion electrons. In fact, it is impossible to distinguish only conversion electrons in the energy spectra during the nuclear α decay. It is conceivable that the process of direct ionization by α particles of K shells of daughter atoms produced during the α decay may provide the predominant contribution to the electron spectrum.

The problem of inner shell ionization during α decay has a long history. The process of K-shell ionization during α decay was predicted by Migdal in 1941 [4]. This process was confirmed experimentally only in the early 1950s. The α decay of $^{210}_{84}$Po was studied in the experiments. The experimental values of the K-shell ionization probability were found to be in excellent agreement with theoretical estimations by Migdal [4]. However, after appearance a number of elaborate calculations (see, e.g., short reviews of theoretical and experimental works in Refs. [5–7]), it was inferred that the agreement was accidental. This was associated mainly with the erroneous assumption in Ref. [4] that the ionization was caused by only the effective dipole field produced by the α-particle charge and nuclear charge during α decay while the more important monopole contribution was mistakenly neglected. There are a variety of other drawbacks in the paper by Migdal [4] which are thoroughly considered in Refs. [5,6].

The well-known "fully quantum treatment of ionization in α decay" (see, e.g., [6]) was carried out for the first time by Anholt and Amudsen [8]. Their treatment includes the tunneling of α particles through the Coulomb barrier. The emitted α particle was represented by an outgoing wave function which was matched to the wave function inside the nucleus at the nuclear radius. The total amplitude for K-shell ionization was expressed [8] in terms of the quantum α-particle tunneling amplitude and the standard quantum-semiclassical amplitude for the ionization process from the Coulomb barrier to infinity. The quantum-semiclassical amplitude was calculated in the sudden approximation using a classical trajectory for α particle.

Our consideration of the inner-shell ionization probability during α decay was performed on the basis of a similar quantum mechanical approach. It should be noted that all formulas

were obtained in our paper because detailed expressions were not presented in Ref. [8]. The α-particle tunneling through the atomic barrier was taken into account accurately as distinct from approximations used in Ref. [8].

The electron wave functions for the initial and final states were approximated in Ref. [8] by Dirac hydrogenic wave functions. However, it is known that an adequate consideration of electron wave functions is of importance in calculations of many processes. In particular, use of the Dirac-Fock (DF) method for finding a discrete function as well as a continuum wave function in ICC calculations at low electron energies results in excellent agreement with experimental data [9,10]. As will be shown below, it is low electron energies that make a major contribution to the probability of K-shell ionization following α decay. Because of this we use electron wave functions obtained in the framework of the DF method which allows for a screening of the nuclear electric field by atomic electrons and includes the exact exchange interaction between electrons.

In Secs. II and III, we describe methods, basic formulas, and a number of computational details used in calculations. In Sec. IV, results obtained for the K-shell ionization probability during α decay of five isotopes of $_{84}$Po are considered at length. The results are compared with available experimental values and with previous calculations [8]. New calculations for the α decay of $^{222}_{86}$Rn and the superheavy nuclei $^{249}_{100}$Fm, $^{253}_{102}$No, and $^{272}_{111}$Rg are also presented. All calculations have been performed using our package of computer codes RAINE [11].

II. BASIC FORMULAS

We consider ionization of an inner shell during α decay within the united atom approximation [8], which is consistent with prescription used by Andersen *et al.* [12]. The probability $P_i(Q_\alpha)$ of ith shell ionization at the α-particle energy Q_α is obtained as a result of integration over the final electron energy E_f of the differential probability $dP_i(E_f)/dE_f$. After averaging over initial electron states and summation over final states, the differential probability may be written as

$$\frac{dP_i(E_f)}{dE_f} = (Z_1\alpha)^2(2j_i+1)(2\ell_i+1) \times \sum_L \sum_{\kappa_f} \frac{(2j_f+1)(2\ell_f+1)}{(2L+1)^2}\left(C^{L0}_{\ell_i 0 \ell_f 0}\right)^2 \times W^2(\ell_i j_i \ell_f j_f; 1/2\, L)\left|\tilde{H}^{(L)}_{if}\right|^2. \quad (1)$$

In Eq. (1), Z_1 is the α-particle charge, α is the fine structure constant, ℓ and j are the orbital and total angular momenta of the active electron, respectively, L is the multipolarity of the radiation field, $\kappa = (\ell - j)(2j+1)$ is the relativistic quantum number, $C^{L0}_{\ell_i 0 \ell_f 0}$ is the Clebsch-Gordan coefficient, and $W(\ell_i j_i \ell_f j_f; 1/2\, L)$ is the Racah coefficient. Subscripts i and f refer to the initial (bound) and final (continuum) electron state, respectively. The matrix element $\tilde{H}^{(L)}_{if} = H^{(L)}_{if}/Z_1$. We use relativistic units where the electron Compton wavelength $\hbar/m_0c$ serves as unit of length and the electron rest mass m_0c^2 serves as unit of energy.

The matrix element $H^{(L)}_{if}$ without considering the α-particle tunneling through the atomic barrier may be written as

$$H^{(L)}_{if} = Z_1\left[\frac{1}{\omega}\int_0^\infty \sin(\omega t)\dot{R}(t)\frac{d\tilde{\mathcal{G}}^{(L)}_{if}(R)}{dR}dt - \delta_{L,1}\frac{Z_2}{M_2}I^{(1)}_{if}\int_0^\infty \cos(\omega t)\frac{1}{R^2(t)}dt\right] + iZ_1\left\{\frac{1}{\omega}\int_0^\infty \cos(\omega t)\dot{R}(t)\frac{d\tilde{\mathcal{G}}^{(L)}_{if}(R)}{dR}dt + \delta_{L,1}\frac{Z_2}{M_2}I^{(1)}_{if}\int_0^\infty \sin(\omega t)\frac{1}{R^2(t)}dt + \frac{1}{\omega}\left[\tilde{\mathcal{G}}^{(L)}_{if}(R_0) - \delta_{L,0}I^{(-1)}_{if}\right]\right\}, \quad (2)$$

where $\omega = E_f + \varepsilon_i$ is the electron transition energy and ε_i is the ith shell eigenvalue. It should be noted that the perturbation Hamiltonian in Ref. [8] involves the well-known recoil term. The recoil term is also taken into account in our calculations. In Eq. (2), the second term in squared brackets of the real part and the second term in curly brackets of the imaginary part are associated with the recoil effect.

The time function $\dot{R}(t)$ involved in Eq. (2) is related to the α-particle trajectory over time $R(t)$ from the atomic Coulomb barrier with the radius R_0 to infinity in the following way [7]:

$$\dot{R}(t) = v\left[1 - \frac{R_0}{R(t)}\right]^{1/2}, \quad (3)$$

their values at $t = 0$ being equal to

$$R(0) = R_0; \quad \dot{R}(0) = 0. \quad (4)$$

In Eq. (3), v is the final velocity of the α particle.

The relativistic radial form factor $\tilde{\mathcal{G}}^{(L)}_{if}(R)$ takes the form,

$$\tilde{\mathcal{G}}^{(L)}_{if}(R) = \frac{1}{R^{L+1}}\int_0^R r^L[G_i(r)G_f(r) + F_i(r)F_f(r)]dr + R^L\int_R^\infty \frac{1}{r^{L+1}}[G_i(r)G_f(r) + F_i(r)F_f(r)]dr. \quad (5)$$

Integrals $I^{(1)}_{if}$ and $I^{(-1)}_{if}$ in Eq. (2) are given by

$$I^{(1)}_{if} = \int_0^\infty r[G_i(r)G_f(r) + F_i(r)F_f(r)]dr, \quad (6)$$

$$I^{(-1)}_{if} = \int_0^\infty \frac{1}{r}[G_i(r)G_f(r) + F_i(r)F_f(r)]dr. \quad (7)$$

In Eqs. (5)–(7), $G(r)$ and $F(r)$ are the large and small components of the Dirac electron wave function multiplied by r. Electron wave functions are calculated in the framework of the DF method, that is, the bound and continuum wave functions represent the solutions of the DF equations with exact consideration of the exchange interaction between bound atomic electrons as well as between bound and free electrons [3,11,13]. The bound electron wave functions are normalized

so that

$$\int_0^\infty \left[G_i^2(r) + F_i^2(r)\right]dr = 1. \tag{8}$$

The continuum electron wave functions are normalized per unit energy range.

In the special case of the K shell ($i = 1s$), taking into consideration that only multipoles $L = 0$ and $L = 1$ make a predominant contribution, Eq. (1) is simplified to the following form:

$$\frac{dP_K(E_f)}{dE_f} = (Z_1\alpha)^2\left[2\left|\tilde{H}^{(L=0)}_{1s\,E_f s_{1/2}}\right|^2 + \frac{2}{9}\left|\tilde{H}^{(L=1)}_{1s\,E_f p_{1/2}}\right|^2 + \frac{4}{9}\left|\tilde{H}^{(L=1)}_{1s\,E_f p_{3/2}}\right|^2\right]. \tag{9}$$

To take into account the α-particle tunneling through the atomic Coulomb barrier, an additional term $a_{if}^{(L)}(E_f)$ has to be included in the imaginary part of $H_{if}^{(L)}$ in Eq. (2). According to the treatment [8], the tunneling term may be written in our notation as follows:

$$a_{if}^{(L)}(E_f) = -i\frac{R_0}{v}\int_{x_0}^1 \frac{x\,dx}{\sqrt{x-x^2}} b_{if}^{(L)}(xR_0) \times \exp\left(\omega\frac{R_0}{v}\int_1^x \frac{x'dx'}{\sqrt{x'-(x')^2}}\right), \tag{10}$$

where $x_0 = R_{\rm nucl}/R_0$ and $R_{\rm nucl}$ is the nuclear radius. In Ref. [8], authors used a number of approximations to estimate the tunneling term $a_{if}^{(L)}(E_f)$. We have obtained exact formulas for coefficients $b_{if}^{(L)}$ on the basis of the relevant expression from [8] (see Eq. (27) in Ref. [8]). The exact values of $b_{if}^{(L)}$ for $L = 0$ and $L = 1$ have the following forms:

$$b_{if}^{(L=0)}(R) = \tilde{\mathcal{G}}_{if}^{(L=0)}(R) - I_{if}^{(-1)}, \tag{11}$$

$$b_{if}^{(L=1)}(R) = \tilde{\mathcal{G}}_{if}^{(L=1)}(R) + I_{if}^{(1)}\omega^2 R\left(\frac{1}{Z_2} - \frac{\mu}{M_2 Z_1}\right). \tag{12}$$

In addition, the integral in the exponent of Eq. (10) was calculated analytically with the result [14],

$$\int_1^x \frac{x'dx'}{\sqrt{x'-(x')^2}} = -\frac{\pi}{4} - \sqrt{x-x^2} - \frac{1}{2}\arcsin(1-2x). \tag{13}$$

Therefore the tunneling term becomes equal to

$$a_{if}^{(L)}(E_f) = -i\frac{R_0}{v}\int_{x_0}^1 \frac{x\,dx}{\sqrt{x-x^2}} b_{if}^{(L)}(xR_0) \times \exp\left[-\omega\frac{R_0}{v}\left(\frac{\pi}{4} + \sqrt{x-x^2} + \frac{1}{2}\arcsin(1-2x)\right)\right]. \tag{14}$$

In our calculations of the ionization probability, the exact tunneling term $a_{if}^{(L)}$ was included in the matrix element $H_{if}^{(L)}$ in the form of Eq. (14) which differs from the approximate term in Ref. [8]. The method for the accurate calculation of the integral (14) is described in detail in Sec. III.

III. METHODS OF CALCULATION

Here we describe a number of essential details applied in our numerical calculations. We denote the α-particle mass by M_1. The charge and mass of the daughter nucleus generated by the α decay of the parent nucleus with a charge Z and a mass number A are equal to $Z_2 = Z - Z_1$ and $M_2 = A - M_1$. The final velocity of the α particle may be found using the expression,

$$v = \sqrt{\frac{2Q}{\mu}}, \tag{15}$$

where μ is the reduced mass and $Q = Q_\alpha - \omega$. The Coulomb radius R_0 is given by

$$R_0 = \frac{Z_1 Z_2 \alpha}{Q}. \tag{16}$$

Further, the α-particle trajectory $R(t)$ from the Coulomb barrier to infinity may be defined in terms of the parameter θ using the following expressions for $R(\theta)$ and $t(\theta)$ [7]:

$$R(\theta) = \frac{1}{2}R_0(1+\cosh\theta), \tag{17}$$

$$t(\theta) = \frac{1}{2}\frac{R_0}{v}(\theta + \sinh\theta). \tag{18}$$

We use an equidistant mesh over time t in the range $0 \leqslant t \leqslant t_{\rm max}$ where

$$t_{\rm max} = \frac{R_{\rm max}}{v}. \tag{19}$$

The maximal distance $R_{\rm max}$ is chosen in our calculations in accordance with the expected value for the outermost atomic shell. In the case of $_{84}$Po, the value was assumed to be $R_{\rm max} = \frac{1}{3} < r >_{6p} \approx 1$ a.u. It was verified that increasing $R_{\rm max}$ by a factor of 6 does not change values of $dP_K(E_f)/dE_f$. A number $N_{\rm p}$ of points t is chosen depending on the energy E_f so that 20 points are placed in each a half-period of the oscillation of $\cos(\omega t)$ or $\sin(\omega t)$ [see Eq. (2)], $N_{\rm p}$ being $\geqslant 16001$.

Values of θ_i are found in points t of the mesh solving transcendental Eq. (18) by the tangent method where the jth approximation to the ith root is found as

$$\theta_i^{(j)} = \theta_i^{(j-1)} - \frac{R_0\left[\theta_i^{(j-1)} + \sinh\theta_i^{(j-1)}\right] - 2vt_i}{R_0\left[1+\cosh\theta_i^{(j-1)}\right]}. \tag{20}$$

Using Eqs. (18) and (20), one may calculate values of θ_i and then obtain the trajectory $R(t)$ with Eq. (17) as well as values of $\dot{R}(t)$ involved in Eq. (2).

To calculate the relativistic form factor $\tilde{\mathcal{G}}_{if}^{(L)}(R)$ [Eq. (5)], we introduce functions $Z_L(r)$ and $Y_L(r) \equiv \tilde{\mathcal{G}}_{if}^{(L)}(R)$ as follows:

$$Z_L(r) = r^{-(L+1)}\int_0^r (r')^L[G_i(r')G_f(r') + F_i(r')F_f(r')]dr', \tag{21}$$

$$Y_L(r) = Z_L(r) + r^L\int_r^\infty (r')^{-(L+1)} \times [G_i(r')G_f(r') + F_i(r')F_f(r')]dr'. \tag{22}$$

The form factor involves the continuum wave function which behaves in the asymptotic region as e^{ipr} where $p = \sqrt{E^2-1}$ and E is the total electron energy including the rest energy. Therefore functions $Z_L(r)$ and $Y_L(r)$ are conveniently calculated in points of a semilogarithmic mesh. The mesh is defined so that at small r, its nodes are close to the nodes of the logarithmic mesh used in our DF calculations for bound wave functions:

$$r_i = r_0 e^{\nu(\tau_i - 1)}, \tag{23}$$

where $r_0 = 0.006\,\hbar/m_0c$, $\nu = 0.04$, and $\tau_i = 1,2,3....$ At large r, the semilogarithmic mesh is close to the uniform one and has to include the preassigned number of points M within one oscillation period of the continuum wave function, that is,

$$pM(r_{i+1} - r_i) \approx 2\pi. \tag{24}$$

Consequently, the semilogarithmic mesh depends on the continuum electron energy E_f.

Let us introduce the following change of variables:

$$\tau_i = \beta r_i + \frac{1}{\nu}\ln(r_i/r_0) + 1. \tag{25}$$

To meet the requirement (24), the parameter β is chosen as

$$\beta = \frac{pM}{2\pi}, \tag{26}$$

parameters r_0 and ν being the same as indicated above. To calculate mesh nodes, one has to find roots of the transcendental algebraic equation (25). Using new variables τ, functions Y_L and Z_L satisfy the system of differential equations,

$$\frac{dZ_L}{d\tau} = \{-(L+1)Z_L + [G_i(r)G_f(r) + F_i(r)F_f(r)]\}\frac{\nu}{\beta\nu r + 1}, \tag{27}$$

$$\frac{dY_L}{d\tau} = [-(2L+1)Z_L + LY_L]\frac{\nu}{\beta\nu r + 1}, \tag{28}$$

as well as boundary conditions,

$$Z_L(r)_{r\approx 0} \approx \frac{r[G_i(r)G_f(r) + F_i(r)F_f(r)]}{L + |\kappa_i| + |\kappa_f| + 1}, \tag{29}$$

$$Y_L(r)_{r\to\infty} \to Z_L(r). \tag{30}$$

The integration of Eqs. (27) and (28) is carried out from left to right and from right to left, respectively, by the use of the Adams four-point method with the following initial conditions for derivatives:

$$\frac{dZ_L}{d\tau_{r\approx 0}} \approx \frac{(|\kappa_i| + |\kappa_f|)[G_i(r)G_f(r) + F_i(r)F_f(r)]}{L + |\kappa_i| + |\kappa_f| + 1} \times \frac{\nu}{\beta\nu r + 1}, \tag{31}$$

$$\frac{dY_L}{d\tau_{r\to\infty}} \to -(L+1)Z_L\frac{\nu}{\beta\nu r + 1}. \tag{32}$$

With Eqs. (21)–(32), we calculate the relativistic form factor $\tilde{\mathcal{G}}_{if}^{(L)}(R)$ in the semilogarithmic mesh along with its derivative which is written as

$$\frac{d\tilde{\mathcal{G}}_{if}^{(L)}(R)}{dR} = \frac{1}{R}\left[L\tilde{\mathcal{G}}_{if}^{(L)}(R) - (2L+1)Z_L\right]. \tag{33}$$

In the form factor calculations, the bound electron wave function of the initial state is found in the self-consistent DF field of the relevant neutral atom while the continuum wave function of the final state is calculated in the field of the ion with the vacancy in the ith shell. The finite nuclear size is taken into account. Inside the nucleus, the potential of a homogeneously charged sphere with radius $R_{\rm nucl} = 1.2A^{1/3}$ fm is assumed.

In closing, it should be noted that an accurate estimation of the integral in Eq. (14) was performed. The integral was calculated using 41 Gauss quadrature nodes and 81 refined nodes [15]. The integration was terminated if the difference between integral values obtained with the Gauss and refined quadratures was less than a prescribed accuracy. If the integral was calculated with an insufficient accuracy, the integration interval should be reduced and the integral should be recalculated. Then the rest of the interval was estimated. This method is efficient and ensures the accuracy required in the calculations.

IV. RESULTS AND DISCUSSION

Calculations of the probability of K-shell ionization following α decay were performed for five polonium isotopes. Only two terms of the radiation field with $L = 0$ and $L = 1$ were included in the sum over L in Eq. (1). We have verified that the term with $L = 2$ contributes less than 1%.

The relativistic form factor $\tilde{\mathcal{G}}_{if}^{(L)}(R)$ was calculated by the DF method at points of the semilogarithmic mesh and then was found by an interpolation into points of equidistant mesh $R(t)$ for using in Eq. (2) and into the Gauss/refined quadrature nodes for using in Eqs. (11) and (12). Form factors $\tilde{\mathcal{G}}_{if}^{(L)}(R)$ are shown in Fig. 1 at the electron energy $E_f = 50$ keV for transitions $1s \to E_f s$ $(L = 0)$ as well as $1s \to E_f p_{1/2}$ $(L = 1)$ and $1s \to E_f p_{3/2}$ $(L = 1)$ in the polonium atom. As is seen, the monopole term considerably exceeds the dipole ones at small values of R and is comparable in magnitude to dipole terms at all larger values of R. The curves are somewhat smooth at this value of E_f and all form factors $\tilde{\mathcal{G}}_{if}^{(L)}(R)$ practically equal to zero at $R \approx 0.2$ a.u.

In Fig. 2, we compare our results with the form factor obtained in Ref. [16] using also the DF method for the $3s \to E_f p_{1/2}$ transition in the palladium atom $(Z = 46)$ in calculations of the ionization probability in atomic collisions at low energy $E_f = 0.1$ keV. One can see that the two curves are very close to each other. There are small differences in extremum ranges of the function $\tilde{\mathcal{G}}_{if}^{(L)}(R)$ where the results are very sensitive to all details of calculations.

To clear up a role of the α-particle tunneling through the Coulomb barrier, we performed calculations of the K-shell ionization probability both taking account for the tunneling and neglecting the tunneling. The differential probability $dP_K(E_f)/dE_f$ is displayed for both cases in Fig. 3. The results are given separately for the monopole term $L = 0$ and the dipole term $L = 1$ as well as for the summary probability $dP_K(E_f)/dE_f$. One can see that in the case when

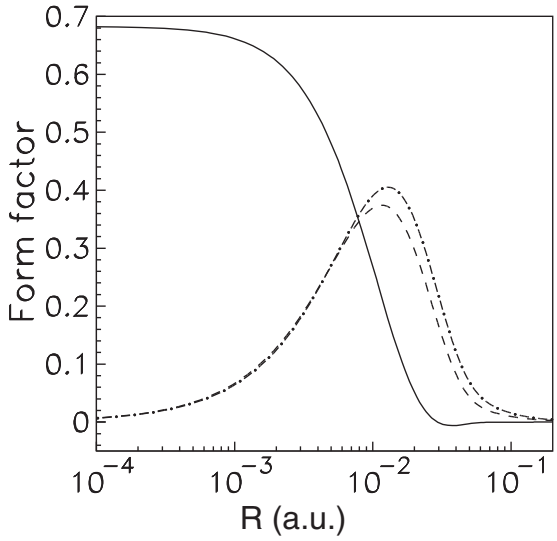

FIG. 1. The relativistic form factor $\tilde{\mathcal{G}}_{if}^{(L)}(R)$ for transitions of the $1s$ electron into continuum states with energy $E_f = 50$ keV in the $_{84}$Po atom. (Solid) $1s \to E_f s$ ($L = 0$); (dashed) $1s \to E_f p_{1/2}$ ($L = 1$); (chain) $1s \to E_f p_{3/2}$ ($L = 1$).

the tunneling is not taken into account, terms with $L = 0$ and $L = 1$ are different in magnitude as well as in behavior. The monopole term is larger at low energies; then it decreases rapidly and becomes nonmonotonic. The dipole term decreases smoothly with energy and becomes larger than the monopole one at energies $E_f \approx 50$ keV. In Fig. 3(a), the solid curve $dP_K(E_f)/dE_f$ drops slowly decreasing only by ~2.5 orders of magnitude at $E_f \approx 1000$ keV. In the case when the tunneling is included [Fig. 3(b)], both curves $L = 0$ and $L = 1$ are smooth and decrease rapidly meeting at point $E_f \approx 160$ keV. The solid curve in this case drops by ~5 orders of magnitude at $E_f \approx 500$ keV. Consequently in this case, the integration over E_f may be performed to several hundred of keV.

On the contrary, the behavior of curves in the case without considering the tunneling [Fig. 3(a)] shows that integration over E_f has to be performed up to very high energies E_f because the solid curve drops slowly and the tail of the curve

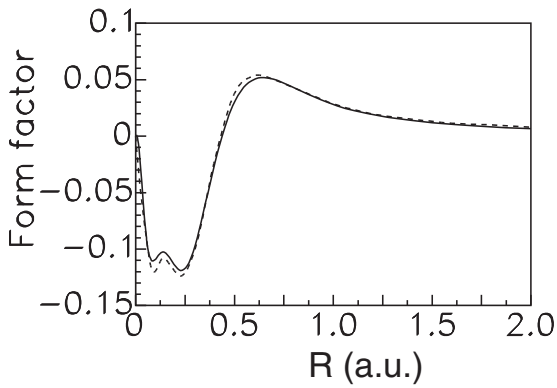

FIG. 2. The form factor $\tilde{\mathcal{G}}_{if}^{(L=1)}(R)$ for transition $3s \to E_f p_{1/2}$ in the $_{46}$Pd atom at $E_f = 0.1$ keV calculated using the DF method. (Solid) Present calculations; (dashed) calculations [16].

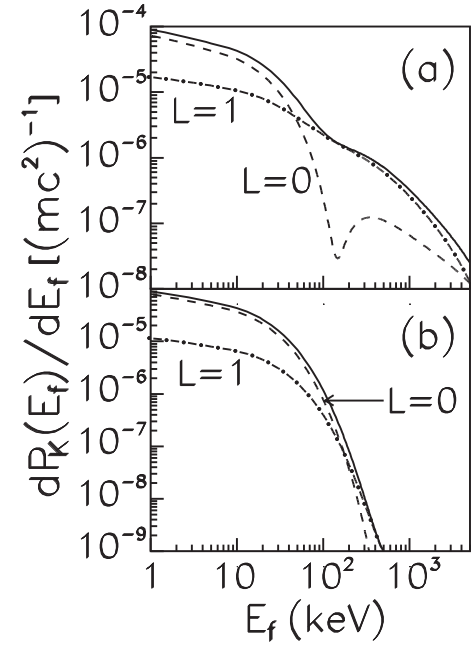

FIG. 3. The differential probability $dP_K(E_f)/dE_f$ for α decay of $^{210}_{84}$Po at $Q_\alpha = 5305$ keV calculated (a) without considering the tunneling and (b) taking into account the tunneling. (Dashed) $L = 0$; (chain) $L = 1$; (solid) sum of the two terms.

may contribute significantly. This is evident from Fig. 4 where we present the value of the integral with the variable upper limit $E_{\rm up}$:

$$P_K(E_{\rm up}) = \int_0^{E_{\rm up}} \frac{dP_K(E_f)}{dE_f} \times dE_f. \tag{34}$$

It is clear that the integral $P_K(E_{\rm up})$ reaches its asymptotic values at $E_{\rm up} \approx 200$–300 keV provided the tunneling is taken

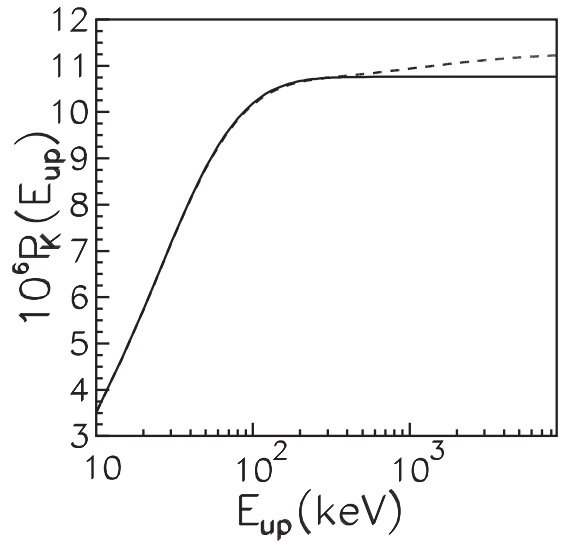

FIG. 4. The integral $P_K(E_{\rm up})$ multiplied by 10^6 for $^{212}_{84}$Po at the α-particle energy $Q_\alpha = 8785$ keV. (Solid) The tunneling is included; (dashed) the tunneling is neglected.

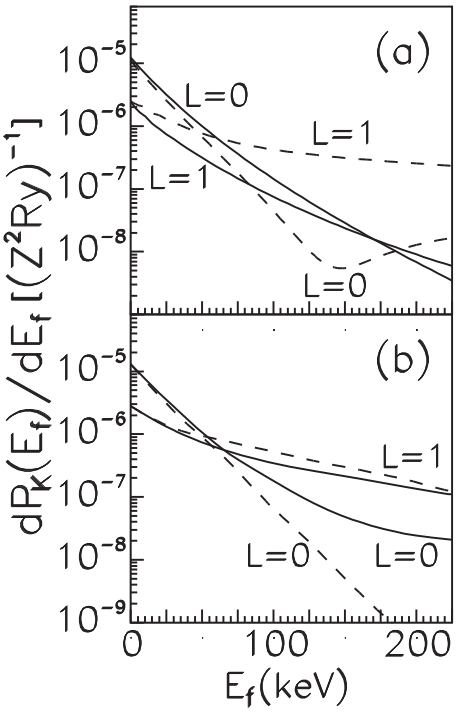

FIG. 5. Components $L = 0$ and $L = 1$ of the differential probability $dP_K(E_f)/dE_f$ for K-shell ionization following the $^{210}_{84}$Po α decay at $Q_\alpha = 5305$ keV obtained (a) in present calculations and (b) in Ref. [8]. (Solid) Calculations including the tunneling; (dashed) without considering the tunneling.

into consideration while in the case without considering the tunneling, the integral practically does not reach an asymptotic value up to the maximal energy $E_{\rm up} = Q_\alpha - \varepsilon_K$. Because of this, we computed the integral over E_f in the latter case up to the value $E_f \approx Q_\alpha - \varepsilon_K$ where $\varepsilon_K = 93.7$ keV for the K shell of the Po atom. In Fig. 4, $P_K(E_{\rm up})$ is displayed only for the isotope $^{212}_{84}$Po with $Q_\alpha = 8785$ keV. We compared the results for isotopes with different energies Q_α. A conclusion can be drawn that in the case without considering the tunneling, the integral $P_K(E_{\rm up})$ retards a growth at high energies E_f when the α-particle energy increases. Consequently, the influence of the tunneling decreases with increasing Q_α.

In Fig. 5, we compare components $L = 0$ and $L = 1$ entering into the differential K-ionization probability $dP_K(E_f)/dE_f$ calculated in the present paper [Fig. 5(a)] and in Ref. [8] [Fig. 5(b)] at α decay of $^{210}_{84}$Po at $Q_\alpha = 5305$ keV in the energy range $E_f \lesssim 225$ keV. Results with allowance made for the tunneling are showed by solid curves. Calculations without considering the tunneling are depicted by dashed curves. Note that shapes of the curves in Fig. 5(a) differ from relevant curves in Fig. 3 because of different scales along the x axis. Presented in Fig. 5(b) are calculations by Anholt and Amundsen [8] where the hydrogenlike electron wave functions of the initial and final states are used and a number of approximations are involved in tunneling calculations.

One can see that the component $L = 0$ is larger than $L = 1$ at low energies in any case. As was mentioned above, our calculations show that in the case where the tunneling is ignored, the two components intersect at $E_f \approx 50$ keV while in the case with taking account for the tunneling, $L = 1$ becomes larger only at $E_f \approx 160$ keV. As is seen from Fig. 5(b), there are similar intersections of the two components in calculations [8]. However, in the case when the tunneling is included, the intersection occurs at $E_f \approx 65$ keV. It is clear from comparison of the two computations that the tunneling makes a small contribution to the dipole term in calculations [8] while in our calculations, the tunneling contribution to the dipole term is considerable even at low electron energies E_f and increases with increasing E_f. Monopole terms also behave in different ways in the two calculations.

TABLE I. Contributions of terms with $L = 0$ and $L = 1$ to the total probability $P_K(Q_\alpha)$ multiplied by 10^6 for isotopes of $_{84}$Po along with experimental values of the probability.

Isotope	Q_α, keV	Experiment	No tunneling		Tunneling	
			$L = 0$	$L = 1$	$L = 0$	$L = 1$
^{210}Po	5305	2.58 ± 0.08 [6]	2.358	2.783	2.458	0.541
^{218}Po	6002	3.73 ± 0.25 [17]	3.341	2.424	3.531	0.778
^{216}Po	6777	4.42 ± 0.4 [6]	4.667	2.270	4.882	1.045
^{214}Po	7687	6.1 ± 0.3 [17]	6.418	2.284	6.631	1.385
^{212}Po	8785	7.4 ± 1.1 [6]	8.743	2.480	8.930	1.829

We present in Table I contributions from terms with $L = 0$ and $L = 1$ to the total K-shell ionization probability $P_K(Q_\alpha)$ obtained in our DF calculations for five isotopes of $_{84}$Po. Table I demonstrates that taking into account the tunneling slightly increases by 2%–5% the monopole term while the

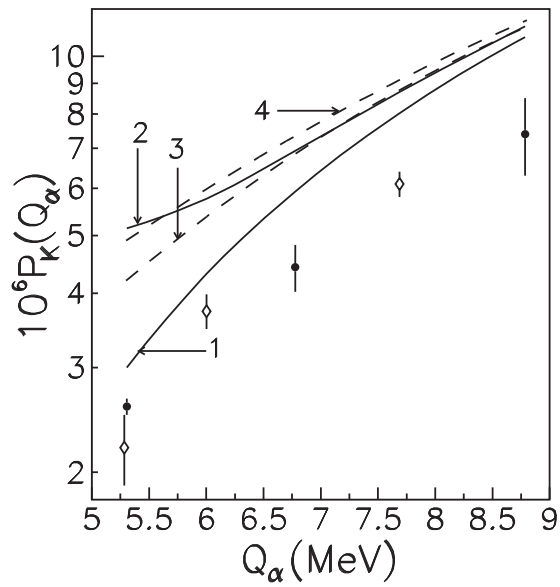

FIG. 6. Ionization probabilities $P_K(Q_\alpha)$ multiplied by 10^6 for the $_{84}$Po isotopes. Present DF calculations: 1, including the tunneling; 2, without considering the tunneling. Previous calculations [8]: 3, including the tunneling; 4, without considering the tunneling. Experimental data as follows: solid circle, Lund *et al.* [6]; open diamond, Eremin *et al.* [17].

TABLE II. Probabilities of K-shell ionization $P_K(Q_\alpha)$ multiplied by 10^6 at α decay of ^{222}Rn and superheavy nuclei.

Parent nucleus	Q_α, keV	$P_K \times 10^6$	Experiment
$^{222}_{86}Rn_{136}$	5490	2.942	2.36 ± 0.22 [17]
$^{249}_{100}Fm_{149}$	7529	3.880	
$^{253}_{102}No_{151}$	8003	4.375	
$^{272}_{111}Rg_{161}$	9630	6.221	
$^{272}_{111}Rg_{161}$	11000	9.125	

dipole term decreases considerably, e.g., by the factor of ∼5 for ^{210}Po at $Q_\alpha = 5305$ keV. The decrease is less for larger Q_α.

Our results for five isotopes of $_{84}$Po with the α-particle energies listed in Table I are compared with available experimental data as well as with calculations [8] in Fig. 6. Solid curves 1 and 2 refer to our DF calculations. Curve 1 was obtained including the tunneling and curve 2 was calculated neglecting the tunneling. Dashed curves 3 and 4 relate to calculations [8] including and neglecting the tunneling, respectively. Experimental data from Lund *et al.* [6] and Eremin *et al.* [17] are shown. As is seen, our calculations without considering the tunneling (curve 2) are somewhat close to results [8] (curves 3 and 4). Curve 1 associated with our calculations taking into account the tunneling is closer to the experiments than results [8]. This may be explained by more accurate calculations, in particular, the more correct calculation of the tunneling and electron wave functions. Comparison between curve 1 and curve 2 demonstrates once again that the tunneling effect decreases as the α-particle energy increases.

The probabilities for K-shell ionization during the α decay of ^{222}Rn as well as the superheavy nuclei ^{249}Fm, ^{253}No, and ^{272}Rg were obtained using the same method of calculation taking into account the α-particle tunneling through the Coulomb barrier. The results are listed in Table II. As is seen, the probability for $^{222}_{86}$Rn correlates with experimental value obtained in Ref. [17].

V. CONCLUSIONS

The K-shell ionization probabilities following α decay in heavy and superheavy nuclei are considered. The theoretical model employed in present calculations is based on the quantum mechanical treatment developed by Anholt and Amundsen [8]. The contribution associated with the α-particle tunneling through the Coulomb barrier in an atom is taken into account accurately. Electron wave functions are calculated in the framework of the relativistic DF method with the exact consideration of the exchange interaction.

Calculations of the K-shell ionization probabilities have been performed for α decay of five isotopes of the $_{84}$Po nucleus at various α-particle energies from the range $5305\,\text{keV} \leqslant Q_\alpha \leqslant 8785\,\text{keV}$ including the α-particle tunneling as well as without considering the tunneling. The contribution from the tunneling to the total ionization probability is shown to be important. Taking into account the tunneling may decrease the dipole term by several times resulting in a considerable decreasing of the ionization probability $P_K(Q_\alpha)$. The tunneling contribution decreases as the α-particle energy Q_α increases.

The results are compared with previous calculations [8] and with available experimental data. It is shown that present results with allowance made for the tunneling of the α particle through the Coulomb barrier correlate better with experimental values than calculations [8]. Our results obtained without considering the tunneling are close to calculations [8].

New calculations on K-shell ionization after α decay of $^{222}_{86}$Rn and the superheavy nuclei $^{249}_{100}$Fm, $^{253}_{102}$No, and $^{272}_{111}$Rg have been performed. The ionization probability $P_K(Q_\alpha)$ after α decay of $^{222}_{86}$Rn with the energy $Q_\alpha = 5490$ keV is in reasonably good agreement with the experimental value [17].

[1] A. Lopez-Martens *et al.*, Phys. Rev. C **74**, 044303 (2006).
[2] A. Lopez-Martens *et al.*, Nucl. Phys. A **852**, 15 (2011).
[3] I. M. Band, M. B. Trzhaskovskaya, C. W. Nestor Jr., P. O. Tikkanen, and S. Raman, At. Data Nucl. Data Tables **81**, 1 (2002).
[4] A. Migdal, J. Phys. USSR **4**, 449 (1941).
[5] L. Kocbach, in *Proceedings of the Nordic Spring Symposium on Atomic Inner Shell Phenomena, Geilo, Norway, 1978*, Vol. 2, edited by J. M. Hansteen and R. Gundersen (University of Bergen, Bergen, Norway, 1978), p. 65.
[6] M. Lund, J. U. Andersen, E. Lægsgaard, and L. Kocbach, http://owww.phys.au.dk/main/publications/PhD/Martin_Lund.pdf.
[7] J. Law, Nucl. Phys. A **286**, 339 (1977).
[8] R. Anholt and P. A. Amundsen, Phys. Rev. A **25**, 169 (1982).
[9] S. Raman, C. W. Nestor Jr., A. Ichihara, and M. B. Trzhaskovskaya, Phys. Rev. C **66**, 044312 (2002).
[10] N. Nica, J. C. Hardy, V. E. Iacob, S. Raman, C. W. Nestor Jr., and M. B. Trzhaskovskaya, Phys. Rev. C **70**, 054305 (2004).
[11] I. M. Band, M. A. Listengarten, M. B. Trzhaskovskaya, and V. I. Fomichev, Computer Program Complex RAINE, Leningrad Nuclear Physics Institute Reports Nos. 289 (1976), 299 (1977), 300 (1977), 498 (1979), 1479 (1989).
[12] J. U. Andersen, E. Laegsgaard, M. Lund, and C. D. Moak, Nucl. Instrum. Methods **132**, 507 (1976).
[13] I. P. Grant, Adv. Phys. **19**, 747 (1970).
[14] I. S. Gradshteyn and I. M. Ryzhik, *Table of Integrals, Series, and Products* (Academic Press, New York, 1965).
[15] A. S. Kronrod, *Nodes and Weights of Quadrature Formulas* (Consultants Bureau, New York, 1965).
[16] Z. Halabuka, W. Perger, and D. Trautmann, Z. Phys. D **29**, 151 (1994).
[17] N. V. Eremin, V. F. Strizhov, A. V. Tulinov, and O. V. Uljanova, IL Nuovo Cimento A **97**, 629 (1987).